Infectious Diseases Diagnosis & Treatment
Sharifin N & Kassim NHN. Infect Dis Diag Treat 9: 276.
www.doi.org/ 10.29011/2577- 1515.100276
www.gavinpublishers.com

OPEN ACCESS

GAVIN PUBLISHERS

Case Report

Erdheim Chester Disease (ECD): A Case of Diagnostic Dilemma

Nadia Sharifin[1*], Noor Haisyah Noor Kassim[1]

[1]Master of Radiology (MRad), Universiti Malaya; Off-campus Based at Hospital Tengku Ampuan Rahimah, Klang, Selangor, Malaysia

[2]Radiologist, Hospital Tengku Ampuan Rahimah, Klang, Selangor Malaysia

***Corresponding authors:** Nadia Sharifin, Master of Radiology (MRad), Universiti Malaya; Off-campus Based at Hospital Tengku Ampuan Rahimah, Klang, Selangor, Malaysia.

Citation: Sharifin N, Kassim NHN (2025) Erdheim Chester Disease (ECD): A Case of Diagnostic Dilemma. Infect Dis Diag Treat 9: 276. DOI: 10.29011/2577-1515.100276.

Received Date: 30 June 2025; **Accepted Date:** 7 July 2025; **Published Date:** 10 July 2025

Abstract

Erdheim-Chester disease (ECD) is a rare type of non-Langerhans cell histiocytosis characterized by abnormal infiltration of multiple organ systems. It commonly affects the bones, lungs, skin, retro-orbital area, central nervous system (CNS), pituitary gland, blood vessels, kidneys, retroperitoneal space, and the heart. This widespread involvement results from the accumulation of lipid-rich, foamy histiocytes that are CD68-positive on immunohistochemical staining. A definitive diagnosis typically requires a combination of imaging findings and histopathological examination.

Keywords: Erdheim-Chester disease (ECD); Retroperitoneal fibrosis

Introduction

The diagnosis of Erdheim-Chester disease is often delayed due to its rarity. Given the diagnostic challenges associated with the disease, this case report focuses primarily on radiologic findings to aid in earlier recognition. We report a case of a 50-year-old Indian woman who presented in our centre with multiple admissions for urosepsis, chronic obstructive uropathy and fluid overload. She had multiple imaging and treatment for two years before being diagnosed with ECD based on adrenal tissue biopsy.

Case Presentation

A 50-year-old female, with underlying type-II diabetes mellitus, hypertension and dyslipidaemia, presented with fever, upper respiratory tract symptoms, right pleuritic chest pain, dysuria, right hypochondriac pain radiating to groin, back pain, bilateral lower limb swelling and reduced effort tolerance for 3-days. She had a history of similar complaints last year with multiple admissions for urinary tract infection (UTI) and had undergone multiple imaging.

On examination upon presentation, she was tachypnoeic with pedal oedema up to mid-shin. The presence of right lung crepitation on auscultation, positive right renal punch, tender right hypochondria and bilateral xanthelasma were also noted. The ECG showed T-inversion V2-V4, I and aVL, therefore she was also treated as having unstable angina. Blood investigations showed microcytic hypochromic anaemia, hypoalbuminemia, deranged renal profile suggestive of acute kidney injury and UFEME of leucocyte(3+) and blood(1+). Blood and urine cultures were negative.

Ultrasound KUB (US KUB) showed bilateral pyonephrosis, which demonstrated moderate hydronephrosis and proximal hydroureter with echogenic debris within, as was seen in the previous ultrasound. Subsequently, a CECT abdomen was performed (Figure 1). Compared with the previous CECT abdomen done last year, it showed similar bilateral moderate hydronephrosis with diffusely thickened enhancing pelvicalyceal and proximal ureteric walls. No renal or ureteric calculi were seen bilaterally. There was associated bilateral perinephric and renal sinus soft tissue thickening and fat stranding, with mildly thickened Gerota and Zuckerkandl fascia. No perinephric or retroperitoneal collections were noted bilaterally. Perivascular soft tissue thickening was also seen involving the IVC, main renal vessels, and the visualised descending and abdominal aorta, with poor luminal contrast within the IVC suspicious for thrombus. There were heterogeneously enhancing bilateral suprarenal lesions with non-visualisation of the

normal adrenal glands. Multiple enlarged paraaortic, perirenal, aortocaval, paracaval, and mesenteric nodes were noted with mesenteric fat streakiness at the root of the mesentery. Bilateral lung bases showed patchy consolidations, ground-glass opacities, and pleural effusion with thickened pleura. The adjacent pericardium also appeared thickened. Due to the bilateral adrenal lesions, a differential diagnosis of disseminated infection (i.e., tuberculosis), malignancy, or adrenal hyperplasia. was given. Repeated urine culture showed Stenotrophomonas Maltophilia. The patient's condition improved with antibiotics; therefore, she was discharged with a plan to repeat imaging six weeks later.

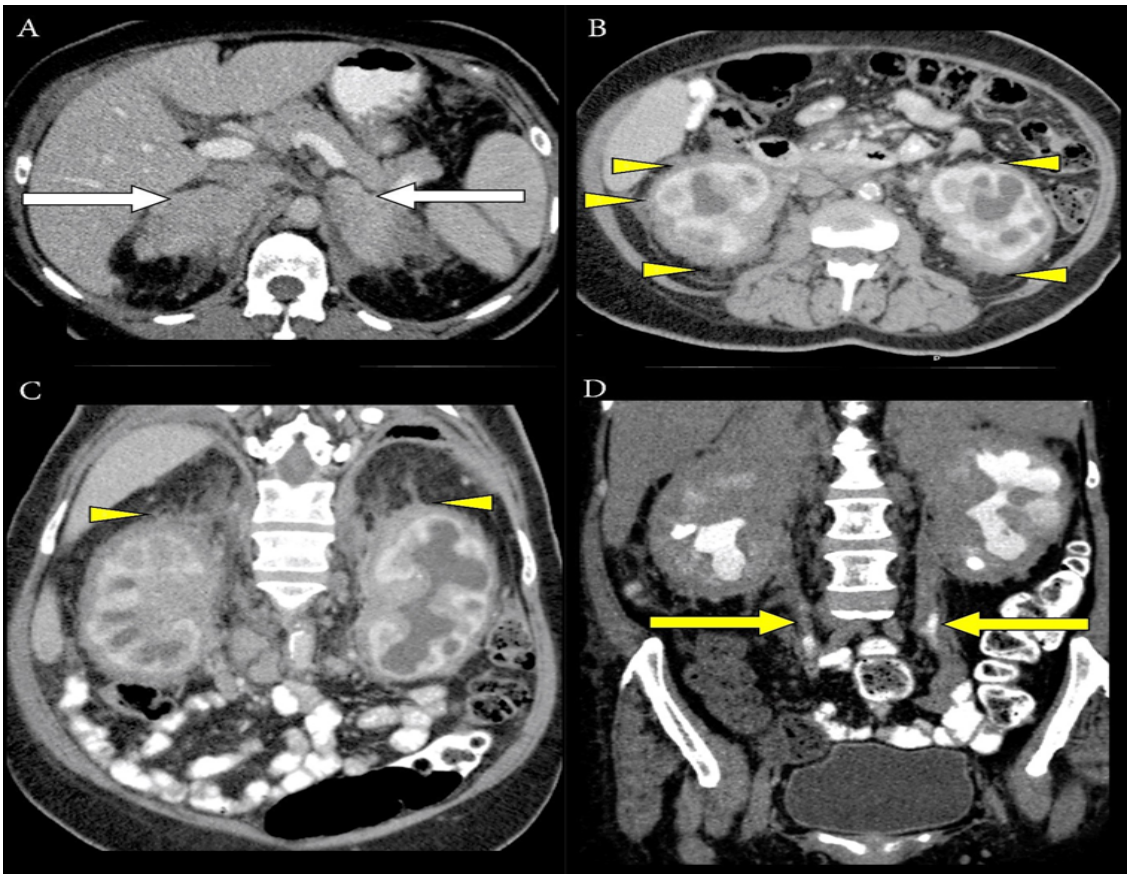

Figure 1: Axial CT image (A) showed heterogeneous enhancement of suprarenal soft tissue lesions with loss of the normal appearance of adrenal glands bilaterally (white arrow). Axial (B) and coronal (C) CT images showed extensive perirenal fat infiltration (yellow arrowhead), causing thickening of the bridging perirenal septa (Kunin septa), and fibrous tissues extended between the renal capsule and perirenal fascia, giving rise to the "hairy kidney" appearance (yellow arrowhead), respectively. Coronal CT image in the delayed phase (D) also showed retroperitoneal soft tissue infiltration involving both proximal and mid ureters (yellow arrow), causing bilateral hydronephrosis.

Unfortunately, she was readmitted with a similar complaint a month later. Pleural tapping was negative for AFB and TB-PCR, whereas culture and sensitivity showed heavily mixed growth. Pleural cytology showed scattered mature lymphocytes and benign mesothelial cells with no malignant cells. Urine culture grew ESBL E. coli, and urine MTB PCR was negative. Repeated ultrasound KUB showed similar findings. CECT TAP was then performed. Findings in the abdomen remained similar, with unchanged bilateral moderate hydronephrosis and extensive enhancing soft tissue thickening at the bilateral suprarenal, perinephric, pelviureteric, and perivascular regions. A moderate right pleural collection was seen, with thickened enhancing pleural lining and collapse-consolidation of the adjacent lung. Cardiomegaly with thickened enhancing pericardial lining and pericardial soft tissue/fluid was seen insinuating the right atrium (Figure 2). Perivascular fluid/soft tissue thickening was also seen at the brachiocephalic artery, subclavian artery at the aortic origin, and periaortic region, with multiple mediastinal nodes.

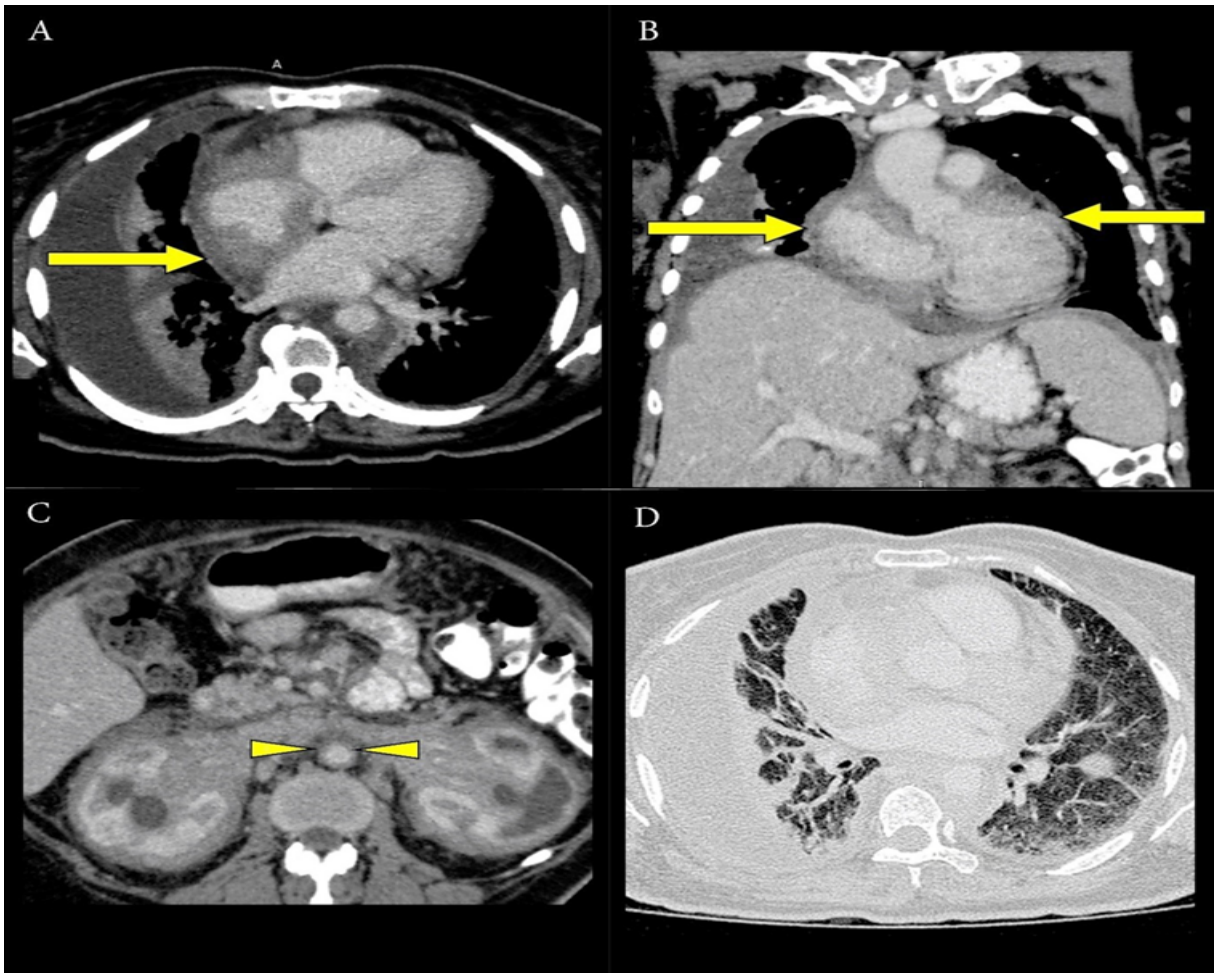

Figure 2: Axial CT image (A) and coronal image (B) showed pericardial infiltration with predominant involvement of the right atrium (yellow arrow). Periaortic soft tissue infiltration (yellow arrowhead) was seen, giving rise to the "coated aorta sign," as demonstrated in axial CT image (C). CT axial image in the lung window (D) showed right pleural effusion with thickening of the interlobular septa and infiltration of the bronchoalveolar bundles, causing fibrosis.

In view of the chronicity and unchanged extensive soft tissue thickening, retroperitoneal fibrosis, and lymphadenopathies seen in imaging performed over a span of two years, underlying systemic causes (i.e., autoimmune or connective tissue disease) were considered, and the differential diagnoses given were lymphoma, Erdheim-Chester disease, and disseminated infection. Autoimmune blood investigations were negative, except for ANA. Tumour markers were also unremarkable. She was discharged with a urology clinic appointment after her condition improved following a two-week course of IV Meropenem.

However, she defaulted to follow-up and presented three months later with similar symptoms and a new onset of atrial fibrillation. ECHO showed a mildly thickened interventricular septum, EF of 62%, PASP of 29 mmHg, and a normal aortic root with no RWMA or LVOT obstruction. Infective markers were again raised, and urine culture grew ESBL Klebsiella pneumoniae. Repeated US KUB and CECT TAP findings remained similar. Following a discussion between the clinician and the responsible radiologist, it was decided that a PET-CT scan should be performed before the biopsy to detect the hotspot location for sampling. The PET-CT scan (Figure 3) showed the presence of FDG-avid disease in the soft tissue of the anterior mediastinum, bilateral adrenal fossae, and retroperitoneal region surrounding both kidneys, bilateral lungs and pleura, spleen, bones, and lymph nodes.

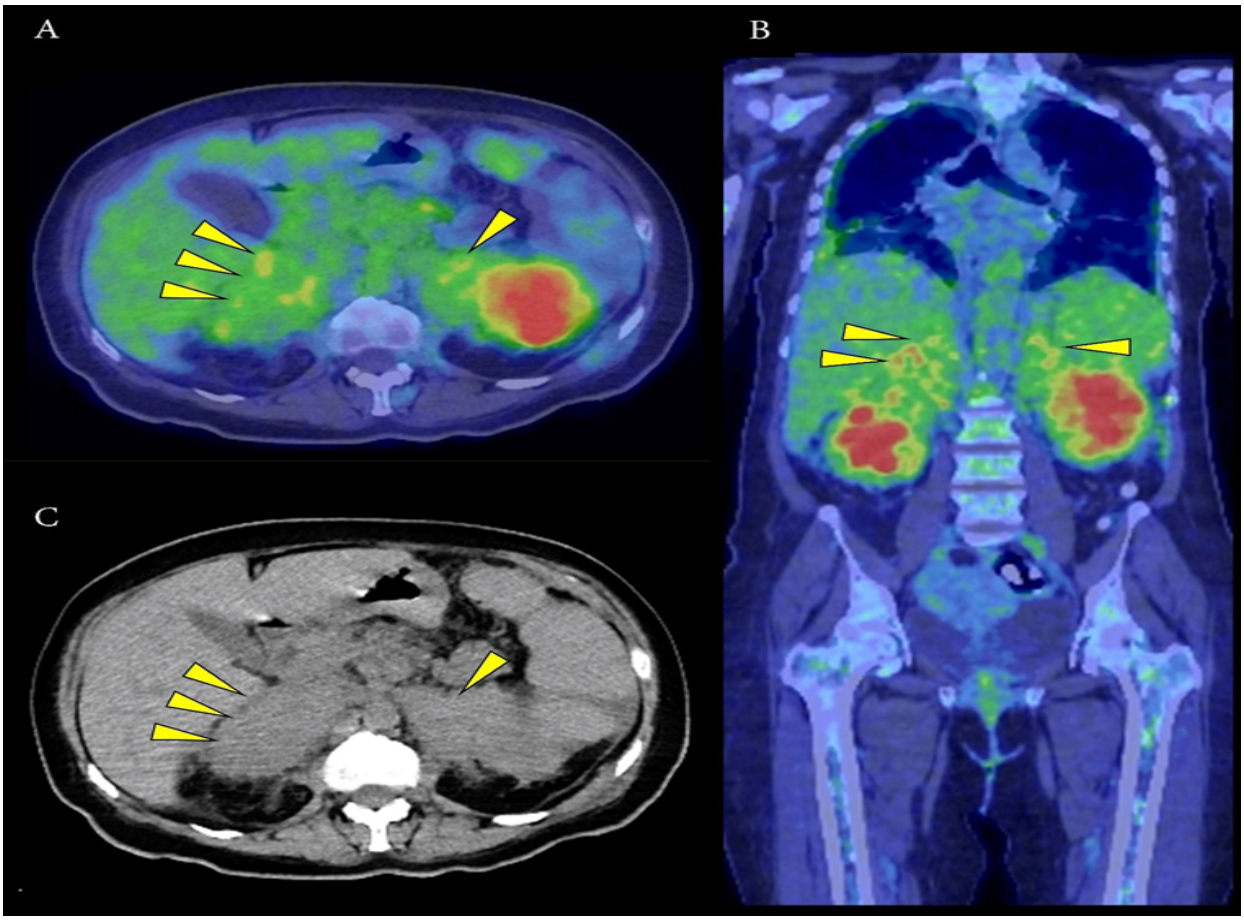

Figure 3: PET-CT scan images in axial (A) and coronal (B) views at the level of the adrenal region showed bilateral uptake (highest SUVmax 8.2 at the right adrenal region). Normal adrenal glands were not visualised in the corresponding CT image (C). Hence, a decision was made to perform a percutaneous CT-guided biopsy of the right adrenal lesion.

HPE results of the adrenal lesion showed scattered clusters of lymphocytes and foamy histiocytes. No amyloid deposition or multinucleated giant cells were seen. Immunohistochemistry staining showed histiocytes CD68(+) and focal S100(+). CD1(−), thus excluding Langerhans cell histiocytosis. Special histochemistry showed no acid-fast bacilli were detected with Ziehl-Neelsen staining. Gene analysis was also positive for the BRAF600E mutation. Based on these results, she was diagnosed with ECD and was treated with high-dose interferon-α, which significantly improved her condition.

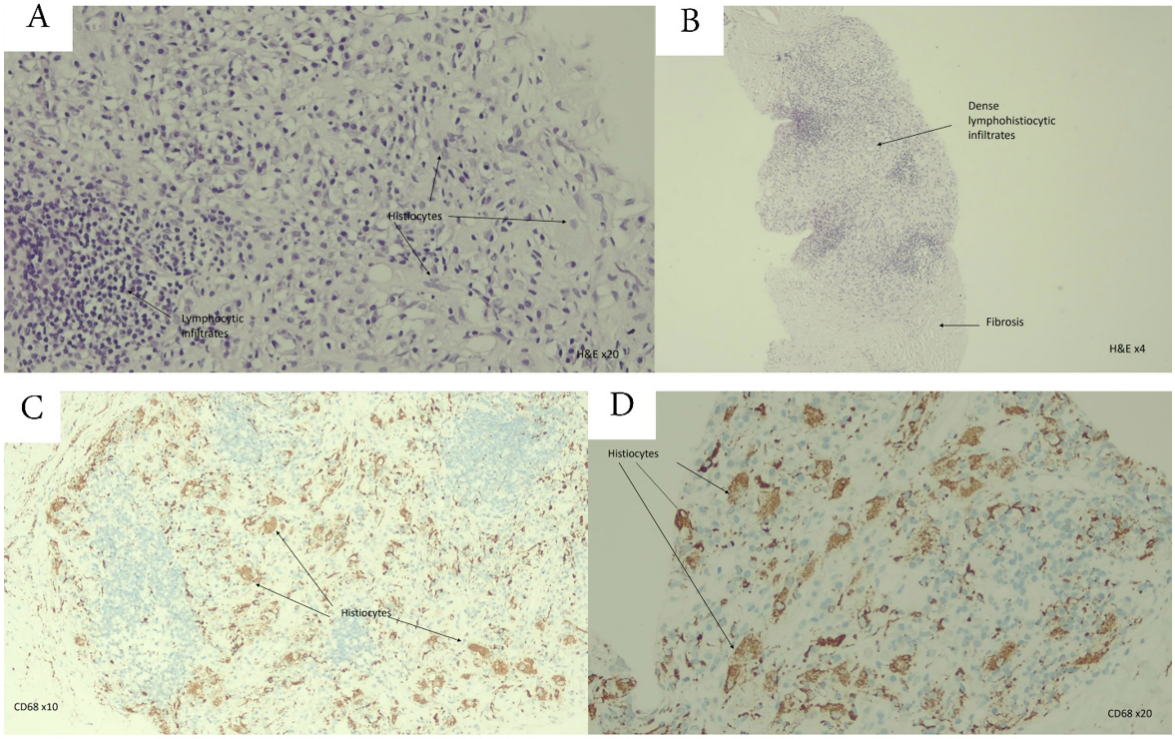

Figure 4: Histopathology images of lesional tissue demonstrated lymphocytic and histiocytic infiltrates (A). Fibrosis was usually present and sometimes predominant, leading to misinterpretation of the lesion as a reactive fibroinflammatory process (B). Immunohistochemistry showed that the histiocytes were positive for CD68 (C, D).

Discussion

Erdheim-Chester disease (ECD) is a rare disorder involving multiple organ systems, marked by xanthomatous infiltration caused by non-Langerhans cell histiocytes. The clinical manifestation depends on the organ affected. There are typical radiographical and pathological features that can lead to the diagnosis. However, due to the rarity of the disease and its broad clinical manifestations, it often causes diagnostic dilemmas, with most initial evaluations and previous imaging resulting in inconclusive diagnoses. We report a case that presented with recurrent urosepsis and chronic obstructive uropathy over 2 years, in which multiple CT scans showed similar findings mainly involving retroperitoneal structures, perivascular areas, pericardium, and lungs.

About 68% of patients report retroperitoneal space involvement, in which most cases are asymptomatic while some are symptomatic, such as dysuria and abdominal pain [1]. There is irregular infiltration involving the bilateral perirenal and posterior pararenal spaces, leading to distorted renal outlines and thickening of the septa of Kunin, which gives rise to the characteristic "hairy kidney" appearance on CT imaging [2]. Extension of the infiltration into the renal sinuses may result in post-renal obstruction. Additionally, associated fibrosis can cause bilateral ureteric obstruction, leading to hydronephrosis and potentially compromised renal function [1]. In most cases, the adrenal glands and surrounding fossae are also affected, which may contribute to adrenal insufficiency [1]. All these imaging findings have been present in our patient over the past 2 years, as demonstrated in Figure 1.

Perivascular involvement, particularly periaortic fibrosis, commonly accompanies infiltration of retroperitoneal structures in ECD. On CT, this manifests as the distinctive "coated aorta" sign, which reflects periaortic fibrotic tissue (Figure 2C). While characteristic, this imaging feature is not unique to ECD. The fibrosis may present as symmetrical or asymmetrical, circumferential or partial, and may involve a segment of the aorta or its full length. This appearance results from histiocytic infiltration of the aortic adventitia. In some cases, the disease may extend to the intimal layer, producing irregular intimal contours on imaging. Similar perivascular involvement can also affect other major vessels, including the coronary arteries, celiac axis, superior mesenteric artery, and renal arteries [1].

Cardiovascular involvement occurs in approximately 75% of patients with ECD, with clinical presentation varying based on the location and extent of the lesions. Among the cardiac manifestations, pericardial infiltration is the most observed. Both periaortic and pericardial involvement can be visualized using CT and echocardiography. On CT imaging, the pericardium may appear thickened, sometimes surrounded by a fibrotic envelope. Myocardial infiltration often follows pericardial involvement and may affect various regions including the ventricular walls, atrial walls, coronary sulcus, and interatrial septum. Around 49% of ECD cases show right heart involvement, with approximately 30% of those exhibiting tumefactive infiltration of the right atrium [3]. In this patient, the clinical symptoms over the past 2 years were primarily related to genitourinary tract involvement. Cardiac symptoms, including unstable angina and later atrial fibrillation, emerged during the last two hospital admissions, most likely due to pericardial infiltration predominantly affecting the right atrium, as demonstrated on contrast-enhanced CT (Figure 2A and 2B).

ECD can present as a form of interstitial lung disease, and pulmonary imaging findings are often non-specific. In the lungs, histiocytic infiltration typically exhibits a lymphangitic distribution, involving the visceral pleura, interlobular septa, and peribronchoalveolar regions, often accompanied by fibrosis, as observed in our patient (Figure 2D**).** The presence of CD68(+), CD1a(−) histiocytes in the bronchoalveolar lavage fluid supports the diagnosis of pulmonary involvement in ECD [1].

When compared to other imaging studies, Arnaud et al. demonstrated that the PET scan exhibits great specificity [4]. We have therefore proposed using a PET-CT scan to locate potential sites for CT-guided percutaneous biopsy in this patient.

Conclusion

Diagnosing ECD poses a great clinical and radiological challenge due to its rarity and multisystemic involvement. Radiological findings aid the clinician; however, tissue biopsy analysis is needed for a definite diagnosis. Therefore, a high index of suspicion is required for further relevant workup and appropriate treatment. In our case, the similar constellation of imaging findings predominantly involving retroperitoneal structures over 2 years raised our suspicion of autoimmune disease, thus leading to further imaging with PET scan and tissue biopsy; these subsequently established a proper diagnosis, treatment, and continuation of care. The significance of this case, however, lies in the inclusion of ECD in the differential diagnosis of retroperitoneal fibrosis to avoid delay in diagnosis.

Declarations

Contributors: All authors contributed to planning, literature review and conduct of the review article. All authors have reviewed and agreed on the final manuscript.

Competing interests: None.

Patient consent for publication: Not applicable.

Ethics approval and consent to participate: Ethical approval for this publication by National Medical Research Register (NMRR), Research ID: RSCH ID-25-03655-ZVH.

Availability of data and materials: Not applicable.

Funding: No Funding.

References

1. Mazor RD, Manevich-Mazor M, Shoenfeld Y (2013) Erdheim-Chester disease: a comprehensive review of the literature. Orphanet J Rare Dis 8:137.
2. Iqbal S (2022) Erdheim-Chester disease [Internet]. Radiopaedia.org; 2022 [cited 2025 Jun 28].
3. Raptis DA, Raptis CA, Jokerst C, Bhalla S (2012) Erdheim-Chester disease with interatrial septum involvement. J Thorac Imaging 27:W105-W107.
4. Arnaud L, Malek Z, Archambaud F, Kas A, Toledano D, et al. (2009) 18F-fluorodeoxyglucose-positron emission tomography scanning is more useful in follow-up than in the initial assessment of patients with Erdheim-Chester disease. Arthritis Rheum 60:3128-3138.
5. Arnaud L, Gorochov G, Charlotte F, Lvovschi V, Parizot C, et al. (2011) Systemic perturbation of cytokine and chemokine networks in Erdheim-Chester disease: a single-center series of 37 patients. Blood 117:2783-2790.
6. Steňová E, Steňo B, Povinec P, Ondriaš F, Rampalová J (2012) FDG-PET in the Erdheim-Chester disease: its diagnostic and follow-up role. Rheumatol Int 32:675-678.